

Local vibrational modes of impurities in diamond

P. J. Lin-Chung

Naval Research Laboratory, Washington, D.C. 20375-5347

(Received 18 July 1994)

Local vibrational modes induced by defect complexes involving nitrogen and silicon impurities in different configurations are calculated using Keating potentials in a supercell model. Both the frequency and the vibrational amplitudes of atoms in the complexes are determined for each mode. It is found that defect complexes involving interstitial impurities produce high-frequency localized modes and substitutional impurities produce low-frequency quasilocated modes. The bond-center Si interstitial is found to have higher lattice energy than the substitutional Si-vacancy pair complex, and hence is less stable. Suggestive atomic models are given based on the present calculations.

I. INTRODUCTION

Experimental research concerning the vibrational modes localized about lattice imperfections has a long history. Theoretical understanding and the controlled preparation of materials with defects, however, has been relatively slow in developing. Local vibrational modes induced by defects in crystals have been observed most frequently using Raman scattering and infrared absorption techniques. Neutron scattering and electron tunneling also shed some light on the defect vibrations. The interaction of the defect center with localized or quasilocated vibrations further produces changes in the optical-absorption and luminescence spectra.¹ In this work we present a theoretical study of the local vibrational modes of impurities in diamond.

Diamond is an interesting material because it has an extreme covalent form of crystal bonding. Unlike the case of Si, optical measurements in diamond probe ground and excited electronic states equally well. Thus the vibronic processes involving both the electrons and vibrational modes can be detected. The high Debye temperature of diamond also enables optical measurements to be made at higher temperatures. Therefore there exist many optical measurements revealing rich structures for different impurity complexes in diamond. We study the local (LM) and quasilocated (QLM) vibrational modes because they affect the spectra of luminescence and absorption and may serve as probes of the defects and their surrounding.

We use a realistic supercell model to find both the frequencies and eigenvectors of the local and quasilocated vibrational modes induced by defects. Knowledge of the eigenvectors is necessary to analyze the atomic vibrations associated with each mode and to determine the symmetry of that mode. The symmetry of a vibrational mode dictates its coupling with certain electronic states and is important information in analyzing the optical data. In this paper we investigate in detail several possible nitrogen complexes and Si complexes in diamond.

II. METHOD

In the present method we construct a supercell which consists of approximately 64 basis atoms.² When the defect complex is placed near the center of such a large supercell the interaction between complexes in different cells becomes negligible. A two-parameter Keating model is used. In such a model the potential at an atom o is expressed in the following form:

$$U = \sum_i \left[\frac{3\alpha_{oi}}{8d_i^2} \right] [(\mathbf{r}_{oi} \cdot \mathbf{r}_{oi}) - d_i^2]^2 + \sum_{i>j} \left[\frac{3\beta_{oij}}{8d_{ij}^2} \right] \left\{ (\mathbf{r}_{oi} \cdot \mathbf{r}_{oj}) + \frac{d_{ij}^2}{3} \right\}^2, \quad (1)$$

where α_{oi} and β_{oij} are the "bond-stretching" force constant between atoms o and i , and the "bond-bending" force constants between the bonds to atoms i and j , centered at atom o , respectively. d_i is the equilibrium bond length between the atoms o and i , and d_{ij}^2 is the product of d_i and d_j .

The bond-stretching force constant α_{oi} and bond-bending force constant β_{oij} for bulk diamond, as listed in Table I, are determined by fitting the bulk diamond phonon dispersion relation. Since a two-parameter fit cannot reproduce the phonon spectrum exactly, the present work is intended to predict the trends of the impurity vibrational modes rather than their exact frequencies. The important zone center and zone boundary phonons calculated for bulk diamond using the present set of force con-

TABLE I. Force-constant parameters (in 10^3 dyn/cm) and equilibrium bond lengths (in Å) used in this calculation.

o	i	j	α_{oi}	β_{oij}	d_{ij}
Si	Si	Si	43.7	11.54	2.351
C	C	C	95.7	63	1.545
C	N	N	97.5	63	1.545

TABLE II. Calculated phonon frequencies at high-symmetry points of the reduced Brillouin zone for pure diamond crystal. (The numbers in the parentheses represent the measured values reported by Warren *et al.*^a)

$(a/2)(k_x, k_y, k_z)$	ω (cm ⁻¹)			
Γ (0,0,0)	Γ_{15} 0 (0)	Γ_{15} 1334.8 (1334)		
X (1,0,0)	X_3 841 (804±34)	X_4 1036.5 (1072±27)	X_1 1115.5 (1183±21)	
L (0.5,0.5,0.5)	L_3 594.7 (552±17)	L_1 945.6 (1035±31)	L'_2 1190.1 (1241±37)	L'_3 1194.9 (1210±36)
W (1,0.5,0)	W_1 901.5 (918±11)	W_1 943.8 (992±53)	W_1 1192.2 (1167±53)	
Δ (0.5,0,0)	Δ_5 497.7 (543.8±16)	Δ_1 661.6 (737±22)	Δ_5 1195 (1215±36)	Δ'_2 1303

^aJ. L. Warren, J. L. Yarnell, G. Dolling, and R. A. Cowley, Phys. Rev. **158**, 805 (1967).

stants are listed in Table II. The phonon spectrum we obtain for diamond is given in Fig. 1. The presence of an impurity complex modifies this spectrum considerably. The modifications which occur below 1334 cm⁻¹ are related to quasilocal modes and those above 1334 cm⁻¹ are called local modes.

The force constants for Si are obtained from the work of Alonso, Cardona, and Kanellis.³ The relevant parameters used in the present calculations are also summarized in Table I. We follow the procedure given in Ref. 2 to interpolate the force-constant parameters and the equilibrium bond lengths between a given pair of atoms which involve the defect atom. Relaxation of the atoms to new equilibrium positions is calculated by minimizing the total strain energy in the supercell. For defect complexes considered here, the relaxation of atoms beyond the second shell of neighbors is found to be less than 1% of the bond length. The atoms at the supercell boundary are virtually unaffected by the relaxation around the defect

atoms. Thus the periodic boundary condition continues to hold in the supercell calculation.

III. RESULTS

In the present study we have considered several impurity complexes involving nitrogen or silicon impurities. Some of the complexes are displayed in Figs. 2 and 3. The

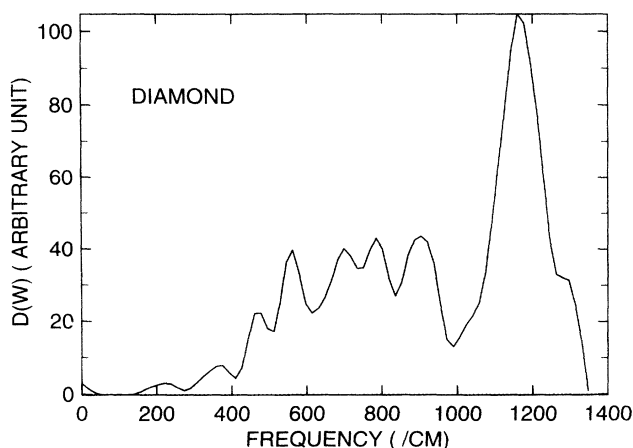


FIG. 1. The calculated phonon spectrum of diamond crystal.

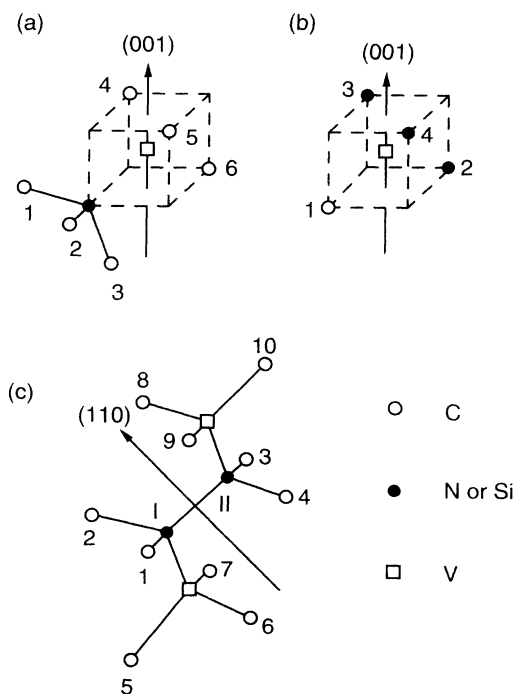


FIG. 2. The atomic configurations of defect complexes in diamond: (a) N₅-V, Si₅-V, or V (with impurity atom replaced by carbon atom), (b) 3N₅-V, and (c) V-N₅-N₅-V. The circle, the square, and the dot represent carbon atom, carbon vacancy, and impurity, respectively.

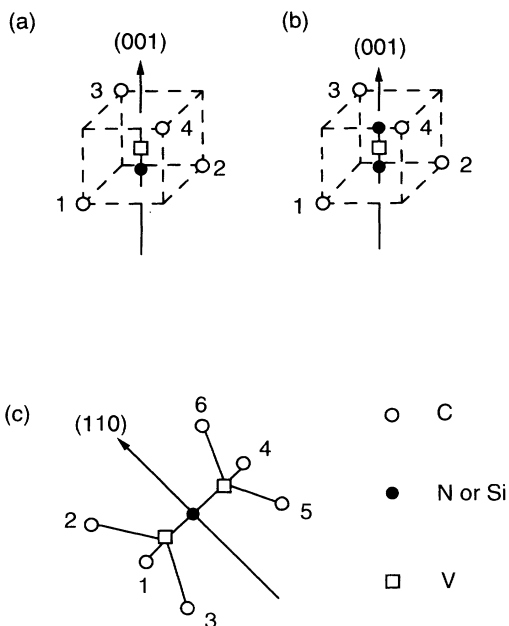


FIG. 3. The atomic configurations of defect complexes in diamond: (a) N_I-V , (b) split interstitials, and (c) $V-Si_I-V$. The circle, the square, and the dot represent carbon atom, carbon vacancy, and impurity, respectively.

vacancy defects are represented by squares. Circles and solid dots represent carbon atoms and impurity atoms, respectively. We shall discuss the interstitial complexes and substitutional complexes in turn.

A. Substitutional complexes

Since the stable complexes always involve a vacancy we first examine the change of the vibrational spectrum due to a single vacancy. For a single isolated vacancy we find several quasilocalized modes at 440.4 cm^{-1} (threefold degenerate), 515.3 cm^{-1} (doubly degenerate), 558 cm^{-1} , and 583.8 cm^{-1} (both nondegenerate). The 558-cm^{-1} mode corresponds to a local vibration involving the breathing mode of the first neighbors of the vacancy. The other modes involve motions of second neighbors as well as first neighbors of the vacancy. The labels of the atomic site listed in all the tables follow the labels in Figs. 2 and 3, respectively, and the relative amplitude of vibration in the (x,y,z) directions are in arbitrary units. The subscripts s and I under the atom labels N and Si in all the tables represent the substitutional and interstitial sites, respectively. For an isolated vacancy, the labels in Table III follow Fig. 2(a), except that the impurity is replaced by a carbon atom C.

Table III lists the displacements of the first neighbors (numbers 4, 5, 6, and C) of the vacancy, and the first neighbors (labeled by 1,2,3) of the C (or N_S , Si_S atom in the cases of $V-N_S$ and $V-Si_S$, respectively). When we decrease the force constants between atoms sitting at the nearest neighbor sites of the vacancy, the corresponding mode frequencies decrease. An outward relaxation of the nearest neighbors decreases the frequencies even further. With a 30% change in the force constants and a relaxa-

tion of the lattice, the breathing mode decreases to 525 cm^{-1} .

When the carbon atom C is substituted by nitrogen and silicon impurities to form $V-N_S$ and $V-Si_S$ complexes, the changes of the mode frequencies are as follows:

$$558 \text{ cm}^{-1} \rightarrow 539.2 \text{ cm}^{-1} \rightarrow 469.9 \text{ cm}^{-1},$$

$$515.3 \text{ cm}^{-1} \rightarrow 511.1 \text{ cm}^{-1} \rightarrow 455.7 \text{ cm}^{-1},$$

$$404.4 \text{ cm}^{-1} \rightarrow \{431.8 \text{ cm}^{-1}, 436.8 \text{ cm}^{-1}\}$$

$$\rightarrow \{340 \text{ cm}^{-1}, 396 \text{ cm}^{-1}\}.$$

In addition to the breathing mode relative to the vacancy, there are other modes which involve large vibrations of atoms 1, 2, 3, and the impurities. The lowest QLM associated with a single isolated vacancy, 404.4 cm^{-1} , also involved the motion of atoms 1, 2, and 3. This mode moves to lower frequency, and the triple degeneracy is split, when the carbon atom is replaced by either a nitrogen or silicon impurity. The $V-N_S$ complex produces several QLM's, as given in Table III, and is believed to give rise to the 638-nm photoluminescence (PL) line.⁴

We also calculate the vibrational modes of an isolated substitutional nitrogen impurity. No LM appears. However, if we allow a static trigonal distortion of the lattice conforming to the Jahn-Teller effect in diamond, several LM's appear above 1334 cm^{-1} . When the neighboring atoms of N_S are displaced from their perfect crystal sites by 0.03 nm, the LM's appear at 1407 and 1485 cm^{-1} . The former is doubly degenerate and involves the motions of two of the neighbors of N_S . The latter is nondegenerate and involves the vibrations of N_S and three of its neighbors.

Two other types of nitrogen impurity complexes, $3N_S-V$ and $V-N_S-N_S-V$ [shown in Figs. 2(b) and 2(c)] are believed to give rise to the 415- and 503-nm PL lines,⁵ respectively. The calculated QLM's for these two complexes are given in Tables IV and V. In comparison with the $V-N_S$ complex, $3N_S-V$ has two more nitrogen atoms replacing carbon atoms. The lowest doubly degenerate QLM at 436.8 cm^{-1} for the $V-N_S$ complex moves to 428.4 cm^{-1} for $3N_S-V$, whereas the nondegenerate 431.8-cm^{-1} QLM remains almost the same. When the three N_S atoms move inward toward V in the $3N_S-V$ complex the two lowest modes move to higher frequencies. For the $2N_S-2V$ complex the lowest QLM is at lower energy compared to the previous two cases. As shown in Fig. 2(c), atoms 1,2(3,4) are near neighbors of $N_S(I)$ [$N_S(II)$], and atoms 5,6,7(8,9,10) are near neighbors of the vacancies, respectively. Atoms 5 and 10 are on the same plane as the defect complex. The lowest modes, 369.5 and 424 cm^{-1} , involve motion of the two nitrogen atoms in the same direction, whereas the 434-cm^{-1} mode involves motion in opposite directions. These modes are found to move to lower frequencies, 248.99, 353.4, and 402.7 cm^{-1} , when the nitrogen impurities are replaced by silicon impurities. Detailed analysis of the spectra may serve as a probe of the defect complex type.

TABLE III. The QLM and LM vibrational frequencies and relative vibrational amplitudes of each atom surrounding a single carbon vacancy, and the defect complexes N_S-V and Si_S-V . [The labels of the atoms follow those given in Fig. 2(a).]

	V			
	$440.4 \text{ cm}^{-1} (t)$	$515.3 \text{ cm}^{-1} (d)$	558 cm^{-1}	583.8 cm^{-1}
C	(18,4,22)	(-19,21,-2)	(-23,-23,-23)	(9,13,9)
1	(14,3,15)	(-17,5,-9)	(-9,-4,-9)	(-4,0,-2)
2	(3,0,13)	(-8,10,0)	(-9,-9,-4)	(15,0,-4)
3	(11,3,6)	(-5,17,7)	(-4,-9,-9)	(-3,-2,15)
4	(-18,-4,14)	(-19,-21,2)	(-23,23,23)	(-11,15,11)
5	(-18,-4,-14)	(19,21,2)	(23,-23,23)	(-17,20,-17)
6	(-18,4,-22)	(19,-21,-2)	(23,23,-23)	(14,18,-15)
	N_S-V			
	431.8 cm^{-1}	$436.8 \text{ cm}^{-1} (d)$	$511.1 \text{ cm}^{-1} (d)$	539.2 cm^{-1}
N_S	(28,28,28)	(-1,16,-14)	(8,13,-21)	(28,28,28)
1	(11,12,11)	(-9,8,-11)	(-4,2,-12)	(8,1,8)
2	(11,11,12)	(8,11,-8)	(12,13,-4)	(8,8,1)
3	(12,11,11)	(-1,4,-2)	(0,0,0)	(1,8,8)
4	(-19,0,0)	(-26,-12,13)	(-10,-16,-20)	(22,-22,-22)
5	(0,-19,0)	(26,-15,16)	(-9,13,25)	(-22,22,-22)
6	(0,0,-19)	(1,10,-14)	(7,-16,25)	(-22,-22,22)
	Si_S-V			
	339.5 cm^{-1}	$396.3 \text{ cm}^{-1} (d)$	$455.7 \text{ cm}^{-1} (d)$	469.9 cm^{-1}
Si_S	(-53,-53,-53)	(-50,-4,50)	(-10,26,-16)	(12,12,12)
1	(-9,-3,-9)	(-4,-1,7)	(-5,3,-6)	(-2,-12,-2)
2	(-9,-9,-3)	(-19,-14,14)	(-1,7,-2)	(-2,-2,-12)
3	(-3,-9,-9)	(-12,12,18)	(-1,7,-3)	(-12,-2,-2)
4	(6,2,2)	(7,-10,-9)	(-6,-7,23)	(25,-1,-1)
5	(2,6,2)	(-2,1,0)	(-23,14,-19)	(-1,25,-1)
6	(2,2,6)	(10,11,-8)	(26,0,-8)	(-1,-1,25)

B. Interstitial complexes

There have been absorption and luminescence spectra of neutron-irradiated diamond crystals revealing possible quasilocated vibrational modes associated with either a neutral interstitial carbon atom or to a neutral vacancy at 297, 730 (luminescence), and 333 cm^{-1} (absorption).⁶

It is known that intrinsic interstitials sitting in hexagonal or tetrahedral interstitial sites are unstable. The favorable stable interstitial sites are either the $\langle 100 \rangle$ split interstitial, with one carbon atom removed and two atoms centered on the substitution site, for neutral or singly charged defects, or the bond-centered interstitial for higher positive charges.⁷⁻⁹ Similarly, for impurity defects the stable sites may be the interstitial sites along the C_2 axis, with one C atom removed, and the impurity sitting at the interstitial sites along the C_2 axis [as shown in Figs. 3(a) and 3(b)]. The nitrogen interstitial (N_I) combined with a vacancy (V), shown in Fig. 3(a), has been considered as being responsible for the 575-nm luminescence line.⁵

We assume that the position of N_I in the N_I-V complex given in Fig. 3(a) is $a/4$ above the V along the z direction, where a is the length of the cube edge (not the lattice constant of the crystal). Our calculated results without lattice relaxation produce quasilocal as well as

local modes. The lowest quasilocal modes at 484.22, 489.24, and 577.97 cm^{-1} involve the motion of the N_I atom and the carbon atoms 1 and 2 in Fig. 3(a) in approximately the same direction. (Two of the modes are actually resonant with the bulk modes.) By contrast the local modes at 1340.5, 1354.14, and 1452.05 cm^{-1} involve the motion of the N_I atom against those two carbon atoms.

TABLE IV. The QLM and LM vibrational frequencies and relative vibrational amplitudes of each atom surrounding the defect complex $3N_S-V$. [The labels of the atoms follow those given in Fig. 2(b).]

	$3N_S-V$		
	$428.4 \text{ cm}^{-1} (d)$	432.8 cm^{-1}	$504.7 \text{ cm}^{-1} (d)$
C(1)	(1,-11,10)	(-20,-20,-20)	(18,10,-28)
N_S (2)	(30,14,-16)	(-2,-2,25)	(-9,-4,-27)
N_S (3)	(-2,-11,16)	(25,-2,-2)	(17,-8,17)
N_S (4)	(-30,18,-19)	(-2,25,-2)	(-13,9,17)
	525.5 cm^{-1}	$567 \text{ cm}^{-1} (d)$	577 cm^{-1}
C(1)	(-22,-22,-22)	(-2,4,-2)	(29,29,29)
N_S (2)	(24,24,-25)	(9,13,-11)	(6,6,-2)
N_S (3)	(-25,24,24)	(-13,15,11)	(-2,6,6)
N_S (4)	(24,-25,24)	(-24,25,-24)	(6,-2,6)

TABLE V. The QLM and LM vibrational frequencies and relative vibrational amplitudes of each atom surrounding the defect complex $V-N_S-N_S-V$. [The labels of the atoms follow those given in Fig. 2(c).]

	369.5 cm ⁻¹	424 cm ⁻¹	$V-N_S-N_S-V$ 433 cm ⁻¹	434 cm ⁻¹	468 cm ⁻¹
$N_S(I)$	(9, -37, -37)	(-28, 11, 11)	(18, -14, -14)	(0, 8, -9)	(-25, -20, -20)
$N_S(II)$	(9, -37, -37)	(-28, 11, 11)	(-18, 14, 14)	(0, -8, 9)	(-25, -20, -20)
1	(1, -8, -8)	(-13, 2, -3)	(6, -14, -11)	(-7, 10, -6)	(-14, -2, -2)
2	(1, -8, -8)	(-13, -3, 2)	(6, -11, -14)	(7, 6, -10)	(-14, -2, -2)
3	(1, -8, -8)	(-13, -3, 2)	(-6, 11, 14)	(-7, -6, 10)	(-14, -2, -2)
4	(1, -8, -8)	(-13, 2, -3)	(-6, 14, 11)	(7, -10, 6)	(-14, -2, -2)
5	(-4, 10, 10)	(15, 15, 15)	(-17, -10, -10)	(0, 12, -12)	(3, 1, 1)
6	(3, 9, -8)	(-4, 0, -12)	(-5, 8, 11)	(-13, -16, 14)	(6, -13, 15)
7	(3, -8, 9)	(-4, -12, 0)	(-5, 11, 8)	(13, -14, 16)	(6, 15, -13)
8	(3, -8, 9)	(-4, -12, 0)	(5, -11, -8)	(-13, 14, -16)	(6, 15, -13)
9	(3, 9, -8)	(-4, 0, -12)	(5, -8, -11)	(13, 16, -14)	(6, -13, 15)
10	(-4, 10, 10)	(15, 15, 15)	(17, 10, 10)	(0, -12, 12)	(3, 1, 1)
	480.5 cm ⁻¹	505.4 cm ⁻¹	523.8 cm ⁻¹	931.2 cm ⁻¹	1020 cm ⁻¹
$N_S(I)$	(0, -28, -28)	(-27, 12, 12)	(22, -11, -11)	(-17, -20, -19)	(29, 14, 14)
$N_S(II)$	(0, -28, -28)	(27, -12, -12)	(22, -11, -11)	(17, 20, 19)	(-29, -14, -14)
1	(11, -14, 13)	(-15, 3, 4)	(5, -2, 4)	(-9, 7, -4)	(-5, 9, -9)
2	(-11, -13, 14)	(-15, 4, 3)	(5, 4, -2)	(-9, -5, 7)	(-5, -9, 9)
3	(-11, -13, 14)	(15, -4, -3)	(5, 4, -2)	(9, 5, -7)	(5, 9, -9)
4	(11, -14, 13)	(15, -3, -4)	(5, -2, 4)	(9, -7, 5)	(5, -9, 9)
5	(0, 12, -12)	(-29, -7, -7)	(23, 9, 9)	(5, -6, -6)	(0, 0, 0)
6	(-6, 5, -4)	(-5, -5, -3)	(-19, -7, 12)	(5, 3, 3)	(-2, -3, 2)
7	(6, 4, -5)	(-5, 3, -5)	(-19, 12, -7)	(5, 3, 3)	(-2, 2, -3)
8	(6, 4, -5)	(5, -3, 5)	(-19, 12, -7)	(-5, -3, -3)	(2, -2, 3)
9	(-6, 5, -4)	(5, 5, -3)	(-19, -7, 12)	(-5, -3, -3)	(2, 3, -2)
10	(0, 12, -12)	(29, 7, 7)	(23, 9, 9)	(-5, 6, 6)	(0, 0, 0)

The frequency of each mode and the corresponding vibrational amplitude of each atom for each mode are listed in Table VI.

The 389-nm and the 441.5-nm PL lines were originally considered to arise from the interstitial N_I impurity complex in different configurations.⁵ In this calculation we consider only the split-interstitial N_I impurity complex, with the two N_I atoms located at a distance of $\pm a/4$

from the vacancy V as indicated in Fig. 3(b). The calculated results are given in Table VII. There are three groups of QLM's. The first group, involving mainly motion of the two N_I atoms, has frequencies at 1031 and 1083 cm⁻¹. The second does not involve motion of the N_I atoms. Only the four neighboring carbon atoms [1-4 in Fig. 3(b)] vibrate with frequencies at 1279 and 1341 cm⁻¹. The third group, involving motion of both the N_I

TABLE VI. The QLM and LM vibrational frequencies and relative vibrational amplitudes of each atom surrounding the defect complex N_I-V . [The labels of the atoms follow those given in Fig. 3(a).]

	484.2 cm ⁻¹	N_I-V 489.2 cm ⁻¹	577.9 cm ⁻¹	1257 cm ⁻¹
N_I	(19, 19, 0)	(-17, 17, 0)	(0, 0, -30)	(-24, 24, 0)
1	(15, 15, 6)	(-14, 14, 0)	(1, 1, -26)	(22, -22, 0)
2	(15, 15, -6)	(-14, 14, 0)	(-1, -1, -26)	(22, -22, 0)
3	(-3, -3, 0)	(-4, 4, -10)	(7, -7, 10)	(8, -8, 14)
4	(-3, -3, 0)	(-4, 4, 10)	(-7, 7, 10)	(8, -8, 14)
	1320 cm ⁻¹	1341 cm ⁻¹	1354 cm ⁻¹	1452 cm ⁻¹
N_I	(16, 16, 0)	(-15, 15, 0)	(27, 27, 0)	(0, 0, -57)
1	(-11, -11, -21)	(15, -15, 0)	(-23, -23, -28)	(8, 8, 50)
2	(-11, -11, 21)	(15, -15, 0)	(-23, -23, 28)	(-8, -8, 50)
3	(0, 0, 0)	(10, -10, 8)	(-7, -7, 0)	(0, 0, 5)
4	(0, 0, 0)	(10, -10, -8)	(-7, -7, 0)	(0, 0, 5)

atoms and the four carbon neighbors, has QLM at 1204 cm^{-1} and several LM's at 1400, 1443, 1659, 1668, and 1774 cm^{-1} . The highest LM at 1774 cm^{-1} involves motion of the two nitrogen atoms as a whole in the z direction against the motion of their four neighboring carbon atoms. The calculated results for split C_I interstitials are also listed in Table VII.

The 736-nm (1.681-eV) center observed in Si-ion implanted bulk diamond or electron-irradiated type-IIa diamond is believed to be a complex involving Si.⁵ Several possibilities have been proposed for the 736-nm center. One is associated with the $V\text{-Si}_S$ complex in Fig. 2(a).¹⁰ A related configuration, the $V\text{-Si}_I\text{-V}$ complex shown in Fig. 3(c), where the Si interstitial sits between two vacancies along the (111) direction, may also be possible. The split Si interstitial complex involving two Si atoms is another possibility.⁵ These defect identifications are still not conclusive. The calculated QLM's and LM's for the split Si_I complex are listed in Table VIII. In comparison with the LM's of the three complexes in Tables VII and VIII, we find the following trends of some of the LM's as the C_I 's are replaced by N_I 's and Si_I 's.

$$1834 \text{ cm}^{-1} \rightarrow 1774 \text{ cm}^{-1} \rightarrow 1508 \text{ cm}^{-1},$$

$$1721 \text{ cm}^{-1} \rightarrow 1659 \text{ cm}^{-1} \rightarrow 1495 \text{ cm}^{-1}.$$

Many higher-frequency local modes are found in our calculation for the $V\text{-Si}_I\text{-V}$ complex and are listed in Table IX. However, the calculated lattice energy associated with this bond-center Si interstitial is found to be higher than that of the $\text{Si}_S\text{-V}$ defect. As a result this complex is not stable and the Si_I would move to the vacancy site and form the $\text{Si}_S\text{-V}$ complex.

IV. COMPARISON WITH EXPERIMENTS

The experimental one-phonon absorption spectra of natural type-Ia diamond show defect-induced features. The resonance vibrations (QLM) modify the phonon spectrum of pure diamond, and the LM absorption produces sharp peaks with $\omega > 1334 \text{ cm}^{-1}$. The most prominent features are the B' peak at 1365 cm^{-1} , the 328 cm^{-1} peak, and the component D . They have been interpreted as induced from platelets, bending modes of atom-

TABLE VII. The QLM and LM vibrational frequencies and relative vibrational amplitudes of each atom surrounding defect complexes involving split-N and split-C interstitials. [The labels of the atoms follow those given in Fig. 3(b).]

	1031 cm^{-1} (d)	1083 cm^{-1} (d)	Split N_I 1204 cm^{-1}	1279 cm^{-1} (d)	1341 cm^{-1}
$N_I(1)$	(-23,36,0)	(-21,32,0)	(0,0,23)	(2,2,0)	(0,0,0)
$N_I(2)$	(6,-28,0)	(21,-32,0)	(0,0,-23)	(-6,-6,0)	(0,0,0)
1	(-6,7,2)	(-1,1,0)	(-3,-3,15)	(-20,-13,28)	(27,-27,0)
2	(-6,7,-2)	(-1,1,0)	(3,3,15)	(-20,-13,-28)	(-27,27,0)
3	(0,-4,-6)	(0,0,-2)	(-3,3,-15)	(22,16,5)	(27,27,0)
4	(0,-4,6)	(0,0,2)	(3,3,-15)	(22,16,-5)	(-27,-27,0)
	1400 cm^{-1} (d)	1443 cm^{-1} (d)	1659 cm^{-1}	1668 cm^{-1} (d)	1774 cm^{-1}
$N_I(1)$	(0,0,20)	(-16,8,0)	(0,0,-47)	(31,-7,0)	(0,0,46)
$N_I(2)$	(0,0,-20)	(31,30,0)	(0,0,47)	(40,-26,0)	(0,0,46)
1	(29,29,-5)	(10,-10,37)	(9,9,34)	(-20,-3,-9)	(-10,-10,-34)
2	(-29,-29,-5)	(10,-10,-37)	(-9,-9,34)	(-20,-3,9)	(10,10,-34)
3	(29,-29,5)	(-28,-28,13)	(9,-9,-34)	(-34,28,26)	(10,-10,-34)
4	(-29,29,5)	(-28,-28,-13)	(-9,9,-34)	(-34,28,-26)	(-10,10,-34)
	1115 cm^{-1} (d)	1265 cm^{-1}	Split C_I 1280 cm^{-1} (d)	1341 cm^{-1}	1395 cm^{-1}
$C_I(1)$	(-42,21,0)	(0,0,0)	(-5,-2,0)	(0,0,0)	(0,0,10)
$C_I(2)$	(40,-15,0)	(0,0,0)	(7,5,0)	(0,0,0)	(0,0,10)
1	(-8,7,-3)	(20,-20,0)	(21,11,-29)	(-27,27,0)	(30,30,-10)
2	(-8,7,3)	(-20,20,0)	(21,11,29)	(27,-27,0)	(-30,-30,-10)
3	(5,1,-9)	(-20,-20,0)	(-22,12,-8)	(-27,-27,0)	(-30,30,-10)
4	(5,1,9)	(20,20,0)	(-22,-12,8)	(27,27,0)	(30,-30,-10)
	1431 cm^{-1} (d)	1470 cm^{-1} (d)	1713 cm^{-1} (d)	1721 cm^{-1}	1834 cm^{-1}
$C_I(1)$	(0,0,-20)	(9,6,0)	(-44,-10,0)	(0,0,-53)	(0,0,50)
$C_I(2)$	(0,0,20)	(-37,-36,0)	(-44,10,0)	(0,0,53)	(0,0,50)
1	(-29,-29,-1)	(-4,-2,-39)	(30,15,17)	(7,7,30)	(-10,-10,-32)
2	(29,29,-1)	(-4,-2,39)	(30,15,-17)	(-7,-7,30)	(10,10,-32)
3	(-29,29,1)	(28,28,-1)	(30,-16,-17)	(7,-7,-30)	(10,-10,-32)
4	(29,-29,1)	(28,28,1)	(30,-16,17)	(-7,7,-30)	(-10,10,-32)

TABLE VIII. The QLM and LM vibrational frequencies and relative vibrational amplitudes of each atom surrounding defect complexes consisting of split-N-C and split-Si interstitials. [The labels of the atoms follow those given in Fig. 3(b).]

	1036 cm ⁻¹	1097 cm ⁻¹ (<i>d</i>)	Split (N-C) _I 1341 cm ⁻¹	1394 cm ⁻¹	1427 cm ⁻¹
N _I (1)	(-27,27,0)	(-30,-30,0)	(0,0,0)	(0,0,11)	(0,0,-21)
C _I (2)	(16,-16,-0)	(32,32,0)	(0,0,0)	(0,0,9)	(0,0,21)
1	(-7,7,0)	(0,0,-6)	(-27,27,0)	(32,32,-13)	(-26,-26,2)
2	(-7,7,0)	(0,0,6)	(27,-27,0)	(-32,-32,-13)	(26,26,2)
3	(4,-4,-6)	(6,6,0)	(-27,-27,0)	(-28,28,-9)	(-31,31,1)
4	(4,-4,6)	(6,6,0)	(27,27,0)	(28,-28,-9)	(31,-31,1)
	1443 cm ⁻¹	1469 cm ⁻¹	1682 cm ⁻¹ (<i>d</i>)	1702 cm ⁻¹	1812 cm ⁻¹
N _I (1)	(-33,33,0)	(7,7,0)	(0,0,58)	(19,-19,0)	(0,0,32)
C _I (2)	(3,-3,0)	(-35,-35,0)	(0,0,-38)	(39,-39,0)	(0,0,61)
1	(29,-29,0)	(-4,-4,-40)	(-11,-11,-40)	(-9,9,0)	(-8,-8,-25)
2	(29,-29,0)	(-4,-4,40)	(11,11,-40)	(-9,9,0)	(8,8,-25)
3	(0,0,39)	(27,27,0)	(-5,5,23)	(-32,32,26)	(11,-11,-38)
4	(0,0,-39)	(27,27,0)	(5,-5,23)	(-32,32,-26)	(-11,11,-38)
	450 cm ⁻¹ (<i>d</i>)	644 cm ⁻¹ (<i>d</i>)	Split Si _I 654 cm ⁻¹ (<i>d</i>)	863 cm ⁻¹	1328 cm ⁻¹
Si _I (1)	(-42,-42,-1)	(45,-45,0)	(-20,20,0)	(0,0,-35)	(0,0,0)
Si _I (2)	(-29,-29,-1)	(-27,27,0)	(30,-30,0)	(0,0,35)	(0,0,0)
1	(-15,-15,-6)	(8,-8,0)	(-1,1,0)	(0,0,-4)	(-24,24,0)
2	(-15,-15,6)	(8,-8,0)	(-1,1,0)	(0,0,-4)	(23,-23,0)
3	(-8,-8,0)	(0,0,8)	(2,-2,-3)	(0,0,4)	(-24,-23,0)
4	(-8,-8,0)	(0,0,-8)	(2,-2,3)	(0,0,4)	(23,24,0)
	1348 cm ⁻¹ (<i>d</i>)	1351 cm ⁻¹ (<i>d</i>)	1484 cm ⁻¹ (<i>d</i>)	1494.5 cm ⁻¹	1508 cm ⁻¹
Si _I (1)	(9,-9,0)	(0,0,-10)	(-18,-18,0)	(0,0,-19)	(0,0,25)
Si _I (2)	(0,0,0)	(0,0,10)	(-6,-6,0)	(0,0,19)	(0,0,25)
1	(-23,23,0)	(-24,-24,24)	(32,32,38)	(20,20,38)	(-20,-20,-36)
2	(-23,23,0)	(24,24,24)	(35,35,-45)	(-16,-16,33)	(18,18,-34)
3	(-8,8,-23)	(-20,22,-21)	(-1,0,1)	(18,-18,-36)	(-18,-19,-35)
4	(-8,8,23)	(22,-20,-21)	(0,-2,1)	(-18,18,-36)	(-19,18,-35)

TABLE IX. The QLM and LM vibrational frequencies and relative vibrational amplitudes of each atom surrounding the defect complex V-Si_I-V. [The labels of the atoms follow those given in Fig. 3(c).]

	608 cm ⁻¹	1022 cm ⁻¹	V-Si _I -V 1274 cm ⁻¹ (<i>d</i>)	1415 cm ⁻¹ (<i>d</i>)	1421 cm ⁻¹ (<i>d</i>)
Si _I	(19,19,19)	(20,20,20)	(0,0,0)	(1,-38,38)	(1,-11,9)
1	(11,-6,11)	(2,9,2)	(-14,-14,22)	(-25,5,-39)	(21,5,26)
2	(11,11,-6)	(2,2,9)	(-22,26,-6)	(25,39,-5)	(-16,-24,-4)
3	(-6,11,11)	(9,2,2)	(20,-1,-10)	(0,16,-14)	(0,-10,3)
4	(11,11,-6)	(2,2,9)	(22,-26,6)	(10,20,-6)	(24,40,2)
5	(11,-6,11)	(2,9,2)	(14,14,-22)	(-11,6,-20)	(-33,-2,-43)
6	(-6,11,11)	(9,2,2)	(-20,1,10)	(0,10,-9)	(0,19,-7)
	1475 cm ⁻¹	1616 cm ⁻¹			
Si _I	(0,0,0)	(-29,-39,-39)			
1	(-23,-14,-23)	(20,8,20)			
2	(-23,-23,-14)	(20,20,8)			
3	(-14,-23,-23)	(8,20,20)			
4	(23,23,14)	(20,20,8)			
5	(23,14,23)	(20,8,20)			
6	(14,23,23)	(8,20,20)			

ic bonds in the platelets, and platelet-activated lattice vibrational modes, respectively.^{11,12} From our present results, the lower QLM's of the $V-N_S-N_S-V$ defect correspond to the two nitrogen atoms moving parallel or against each other. Their frequencies are lower than those produced by $V-N_S$. If more $V-N_S$ complexes gather on a plane to form a platelet the planar interaction of the N_S may produce even lower-frequency modes and may be responsible for the observed 328-cm^{-1} mode. Our calculation for substitutional N_S defects, however, has not produced LM's beyond 1334 cm^{-1} . Only a Jahn-Teller distorted system involving N_S or an undistorted system involving interstitial nitrogen defects can produce a high-frequency LM.

The LM features in the infrared absorption have also been studied by isotopic substitution.^{13,14} For type-Ib diamond, a mode at 1344 cm^{-1} was proposed to represent a vibration of carbon atoms surrounding a nitrogen while the nitrogen is stationary. In Tables VII and VIII we find such a mode involving only the vibration of carbon atoms surrounding the split interstitials while the interstitials are stationary. On the other hand, our calculation of a single substitutional nitrogen impurity does not produce such a LM. But it does find a resonance vibration at 1143 cm^{-1} , which involves the nitrogen atom but not its near neighbors. This resonance vibration is to be compared to the observed correlated band peaking at 1130 cm^{-1} .¹⁵ One of the LM's from our calculated results for N_S in a trigonally distorted environment with near neighbors displaced by 0.03 nm also represents a vibration of neighboring carbon atoms only. Its frequency, however, is at 1407 cm^{-1} .

For diamond after irradiation and annealing, absorption lines at 1531 and 1570 cm^{-1} are observed and are attributed to the carbon interstitials in slightly different environments.¹⁶ At even heavier neutron irradiation, a weak line appears at 1924 cm^{-1} .¹ We have calculated only the vibrational modes for split-C interstitials. In the presence of this defect many high-frequency LM's appear. The highest one is at 1834 cm^{-1} . It is expected that in systems with more than two double-bonded carbon interstitials, the LM can increase to even higher frequency.

Two peaks, at 1450 cm^{-1} (in types Ia and Ib) and 1502 cm^{-1} (in type Ib only), are observed after annealing irradiated diamond around 750°C . The former is believed to involve only one nitrogen interstitial.¹⁶ The latter is interpreted as a vibrational stretching mode of the bond between a carbon interstitial and an adjacent substitutional N atom, representing a configuration during the transition to form a N interstitial. For heavily neutron-damaged diamond a third peak develops at 1706 cm^{-1} which has been proposed to arise from a diatomic molecular vibration involving carbon and nitrogen. From our calculated results in Tables V and VI, a single nitrogen interstitial vibration produces a LM at 1452 cm^{-1} . However, in our calculation the interstitial position, as shown in Fig. 3(a), is midway between two layers of atoms along the (001) direction. The LM frequency would depend upon the position of the interstitial. No LM involving only the vibration of the carbon and nitrogen diatomic

molecule is found in the defects considered. But vibrations near the frequency of 1706 cm^{-1} exist for both the split- N_I and the split-(N-C) complexes. In both complexes the vibration involves the cluster of interstitials and their neighbors as given in Table VII.

Lawson *et al.*¹⁷ have examined the LM at 1347.6 cm^{-1} associated with the H2 center. Carbon-carbon vibration was suggested as its origin. The H2 center was considered to be a negatively charged state of the H3 (503-nm) center which consists of aggregated substitutional nitrogens. There have been two models for the H3 center. Davies, Nazare, and Hamer suggested the defect center consists of a pair of nitrogen atoms in next neighbor substitutional sites and a vacancy sitting in their common near neighbor site. The symmetry of this complex is rhombic I .¹⁸ Another model suggested that the center was monoclinic- I symmetry⁵ as shown in Fig. 2(c). Our calculated results for undistorted $V-N_S-N_S-V$ do not produce any LM. Since the observed mode is very close to the phonon spectrum edge, a distorted defect complex with a static trigonal distortion of the neighboring atoms from their crystal sites may easily push the carbon-carbon vibration to higher frequency above the spectrum edge.

The 5RL center discovered in type-IIb semiconducting diamond following irradiation and annealing shows LM peaks at about 1397 and 1911 cm^{-1} in the cathodoluminescence spectrum^{14,19} and at 1219 and 1629 cm^{-1} in the absorption spectrum.²⁰ Isotopic studies show that C_I-C_I vibration is involved in this vibration.¹⁴ Again our calculated LM's of the split-carbon interstitial defect complex (as given in Table VII) have many high-frequency vibrations; the two LM's with both C_I moving in the same direction have frequencies close to the two observed. Quantitative comparison cannot be made as the detailed atomic positions of this defect cluster are not known.

Cathodoluminescence and isotope shift studies of the center with 3.188 eV in diamond imply that such a center probably contains radiation damage products (interstitials) and an isolated nitrogen atom,¹³ or interstitial nitrogen atoms in different configurations.⁵ Six sharp peaks associated with LM are observed at 1357.3 , 1375 , 1425.8 , 1441.9 , 1478.2 , and 1535.5 cm^{-1} . The 1441.9-cm^{-1} peak is found to be related to the vibration of a C-N pair, the other five peaks are related to C-C vibrations.¹³ Our calculations suggest that there must be carbon interstitials involved if the nitrogen is at the substitutional site. Another LM observed at 1856 cm^{-1} under certain annealing processes is proved to come from the di-nitrogen center.¹³ From our calculations only interstitial di-nitrogen can produce such a LM.

As for Si complexes the $2Si_S$ sitting at next neighbor sites and the $2Si_I$ split interstitials have very different QLM's from our calculations. When the $2Si_S$ combine with $2V$ as in Fig. 2(c), the QLM's have even lower frequencies. Photoluminescence studies of the 736-nm (1.681-eV) center reveal three prominent sideband features at 1.618 , 1.558 , and 1.527 eV which correspond to 508 -, 992 -, and 1242-cm^{-1} vibrations.^{10,21} From our calculated results in Table III, the Si_S-V complex suggest-

ed by Clark and Dickerson¹⁰ does not produce any QLM's or LM's near that region of frequencies. Only complexes involving interstitial Si produce these kinds of vibrations, as shown in Tables VIII and IX.

In summary, we find that complexes containing interstitial nitrogens always produce higher-frequency local modes while complexes containing substitutional nitrogens produce low-frequency quasilocal modes. Therefore these defects would affect the phonon sidebands in luminescence spectra quite differently. In these calcula-

tions we provide an understanding of the QLM's and LM's of possible defects by using widely accepted models for some of the nitrogen defects. Because a linear chain model is not adequate to represent the effect of three-dimensional crystal vibrations in LM calculations for large defect complexes, we have carried out supercell calculations using dynamical matrices. Atomic models for experimental results have been suggested based on this work.

¹See the review article by C. D. Clark, A. T. Collins, and G. S. Woods, in *The Properties of Natural and Synthetic Diamond*, edited by J. E. Field (Academic, London, 1992), pp. 36–77.

²P. J. Lin-Chung and C. Y. Fong, *Phys. Rev. B* **35**, 9195 (1987).

³M. I. Alonso, M. Cardona, and G. Kanellis, *Solid State Commun.* **69**, 479 (1989).

⁴C. D. Clark and J. Walker, *Proc. R. Soc. London Ser. A* **334**, 241 (1973).

⁵A. M. Zaitsev, A. A. Gippius, and V. S. Vavilov, *Fiz. Tekh. Poluprovodn.* **16**, 397 (1982) [*Sov. Phys. Semicond.* **16**, 252 (1982)].

⁶D. S. Nedzvetskii and V. A. Gaisin, *Fiz. Tverd. Tela (Leningrad)* **14**, 2946 (1972) [*Sov. Phys. Solid State* **14**, 2535 (1973)].

⁷C. Weigel, D. Peak, J. W. Corbett, G. D. Watkins, and R. P. Messmer, *Phys. Rev. B* **8**, 2906 (1973).

⁸C. Weigel, D. Peak, J. W. Corbett, G. D. Watkins, and R. P. Messmer, *Phys. Status Solidi B* **63**, 131 (1974).

⁹A. Mainwood, F. P. Larkins, and A. M. Stoneham, *Solid State*

Electron. **21**, 1431 (1978).

¹⁰C. D. Clark and C. B. Dickerson, *Surf. Coatings Technol.* **47**, 336 (1991).

¹¹C. D. Clark and S. T. Davey, *J. Phys. C* **17**, 1127 (1984).

¹²G. S. Woods, *Proc. R. Soc. London Ser. A* **407**, 219 (1986).

¹³A. T. Collins and G. S. Woods, *J. Phys. C* **20**, L797 (1987).

¹⁴A. T. Collins, G. Davies, H. Kanda, and G. S. Woods, *J. Phys. C* **21**, 1363 (1988).

¹⁵G. S. Woods, J. A. Wyk, and A. T. Collins, *Philos. Mag. B* **62**, 589 (1990).

¹⁶G. S. Woods, *Philos. Mag. B* **50**, 673 (1984).

¹⁷S. C. Lawson, G. Davies, A. T. Collins, and A. Mainwood, *J. Phys. Condens. Matter* **4**, 3439 (1992).

¹⁸G. Davies, M. H. Nazare, and M. F. Hamer, *Proc. R. Soc. London Ser. A* **351**, 245 (1976).

¹⁹D. R. Wight, Ph.D. thesis, University of London, 1967.

²⁰A. T. Collins and P. M. Spear, *J. Phys. C* **19**, 6845 (1986).

²¹T. G. Bilodeou, K. Doverspike, U. Strom, J. A. Freitas, and R. Rameshan, *Diamond Relat. Mater.* **2**, 699 (1993).